Dosage-dependent regulation of cell proliferation and adhesion through dual β_2-adrenergic receptor/cAMP signals

Ariana Bruzzone,* Aude Saulière,† Frédéric Finana,‡ Jean-Michel Sénard,†,§ Isabel Lüthy,*,[1] and Céline Galés†,[1,2]

*Instituto de Biología y Medicina Experimental, Consejo Nacional de Investigaciones Científicas y Técnicas (CONICET), Buenos Aires, Argentina; †Institut des Maladies Métaboliques et Cardiovasculaires, Institut National de la Santé et de la Recherche Médicale, Université Toulouse III Paul Sabatier, Toulouse, France; ‡Department of Cellular and Molecular Biology, Institut de Recherche Pierre Fabre, Castres, France; and §Department of Clinical Pharmacology, Toulouse University Hospital, Toulouse, France

ABSTRACT **The role of β-adrenergic receptors (β-ARs) remains controversial in normal and tumor breast. Herein we explore the cAMP signaling involved in β-AR-dependent control of proliferation and adhesion of nontumor human breast cell line MCF-10A. Low concentrations of a β-agonist, isoproterenol (ISO), promote cell adhesion (87.5% cells remaining adherent to the plastic dishes following specific detachment *vs.* 35.0% in control, $P<0.001$), while increasing concentrations further engages an additional 36% inhibition of Erk1/2 phosphorylation (p-Erk1/2)-dependent cell proliferation ($P<0.01$). Isoproterenol dose response on cell adhesion was fitted to a 2-site curve (EC_{50}(1): 16.5±11.5 fM, EC_{50}(2): 4.08±3.09 nM), while ISO significantly inhibited p-Erk1/2 according to a 1-site model (EC_{50}: 0.25±0.13 nM). Using β-AR-selective agonist/antagonists and cAMP analogs/inhibitors, we identified a dosage-dependent signaling in which low ISO concentrations target a β_2-AR population localized in raft microdomains and stimulate a G_s/cAMP/Epac/adhesion-signaling module, while higher concentrations engage a concomitant activation of another β_2-AR population outside rafts and inhibit the proliferation by a G_s/cAMP/PKA-dependent signaling module. Our data provide a new molecular basis for the dose-dependent switch of β-AR signaling. This study also sheds light on a new cAMP pathway core mechanism with a single receptor triggering dual cAMP signaling controlled by PKA or Epac but with different cellular outputs.—Bruzzone, A., Saulière, A., Finana, F., Sénard, J.-M., Lüthy, I., Galés, C. Dosage-dependent regulation of cell proliferation and adhesion through dual β_2-adrenergic receptor/cAMP signals. *FASEB J.* 28, 1342–1354 (2014). www.fasebj.org**

Key Words: MCF-10A human breast cell line · Epac · PKA · signaling compartmentalization

β-Adrenergic receptors (β-ARs) are prototypical G-protein-coupled receptors (GPCRs) activated by catecholamines and encompass 3 different subtypes, β_1-, β_2- and β_3-AR, each of which associates with specific physiological actions (1). These receptors preferentially couple to the heterotrimeric G_s protein activating adenylyl cyclase and producing a transient intracellular second messenger cAMP flow that propagates the signal through direct activation of 2 major downstream effectors: protein kinase A (PKA) and the guanine nucleotide exchange protein activated by cAMP (Epac) (2).

Cyclic AMP, either *via* PKA and/or Epac, controls numerous biological functions, many of which are intimately associated with cancer development, such as stimulation (3) or inhibition (4) of cell proliferation, cell differentiation (5), or migration (6–8). Indeed, cAMP/PKA has been shown to participate at the onset and maintenance of adrenal cortex (9) and thyroid neoplasms (10). cAMP production also induces ovarian

Abbreviations: β-AR, β-adrenergic receptor; βCD, β-methyl-cyclodextrin; AC, adenylyl cyclase; AKAP, A-kinase anchoring protein; Bnz, N6-benzoyladenosine-3′,5′-cyclic monophosphate; BRET, bioluminescence resonance energy transfer; CPT, para-chlorophenylthio-2′-*O*-methyladenosine-3′,5′-cyclic monophosphate; Dob, dobutamine; EGF, epidermal growth factor; Epac, exchange protein activated by cAMP; Epi, epinephrine; Erk1/2, extracellular signal-regulated protein kinases 1 and 2; GPCR, G-protein-coupled receptor; ICI, ICI-118,551; ISO, isoproterenol; MAPK, mitogen-activated protein kinase; NE, norepinephrine; N-Epac, Epac-dominant negative; PD, PD98059; PKA, protein kinase A; PKI, PKA inhibitor; Rp, Rp-8-Br-cAMP; Salb, salbutamol

[1] These authors contributed equally to this work.

[2] Correspondence: Inserm U1048, Institut des Maladies Métaboliques et Cardiovasculaires, I2MC, 1, avenue Jean-Poulhès, BP84225, 31432 Toulouse Cedex 4, France. E-mail: celine.gales@inserm.fr

doi: 10.1096/fj.13-239285

This article includes supplemental data. Please visit *http://www.fasebj.org* to obtain this information.

cancer progression (11) *via* a PKA-Src-dependent mechanism (12). By opposition, cAMP promotes growth inhibition in a broad spectrum of human carcinomas (13), fibrosarcomas (14), and leukemia (15). One of the first cellular functions attributed to Epac was its ability to mediate cell adhesion; this occurs essentially *via* Rap1 activation, its cognate downstream effector (16–19). The signaling mechanisms involved in Epac-induced cell adhesion are a matter of great interest, because of its importance in processes such as inflammation and cancer.

The expression of β-ARs, predominantly of the β_2 subtype, has been characterized in several human breast cancer cell lines (20–23) and breast cancer tissue samples (24, 25). The data connecting β-AR and breast cancer still remain controversial, and little is known about the β_2-AR-associated signaling pathways in normal and tumor breast. Several authors suggested the use of β-AR antagonists as a therapeutic option for breast cancer (26, 27). However, an increase of cAMP levels following β_2-AR stimulation has been shown to inhibit the growth of several human breast cancer cells both *in vitro* and *in vivo* (21, 23, 28, 29). We and others have already demonstrated that this inhibition was associated with blockage of the Raf-1/Mek-1/extracellular signal-regulated protein kinases 1 and 2 (Erk1/2) pathway by cAMP-dependent activation of PKA but not of Epac (23, 28). cAMP also inhibits migration of highly invasive MDA-MB-231 cells (6, 7) and the expression of relevant proteins involved in breast cancer metastasis. These effects are mediated by both PKA- and Epac-dependent pathways (30).

β-ARs have also been described in the noncancer breast HBL-100 cell line (31). However, the role of β-AR activation in these cells remains largely unknown. Only 1 recent study described that β-AR activation leads to cAMP production and subsequent polarization of MCF-10A mammary epithelial cells, thus contributing to lumen formation in 3-dimensional cultures (5). In this study the prodifferentiation action of β-AR most likely argues for an antiproliferative effect; however, the β-subtype involved in these effects still remains to be defined.

Taken together, these studies suggest an antiproliferative action of β-ARs in human breast cancer cells and tumors. However, the β subtypes and associated signaling pathways involved and their biological function still remain largely unknown in noncancer breast cell lines. In the present study, we explored the endogenous β-adrenergic regulation of the proliferative/adhesive properties of the nontumor human breast cell line MCF-10A. We identified a dosage-dependent signaling in which low isoproterenol (ISO) concentrations target a β_2-AR population localized in raft microdomains and stimulate a G_s/cAMP/Epac/adhesion signaling module while higher concentrations engage a concomitant activation of another β_2-AR population outside rafts and inhibit proliferation by a G_s/cAMP/PKA-dependent signaling module.

MATERIALS AND METHODS

Drugs and reagents

The cAMP analogs para-chlorophenylthio-2′-*O*-methyladenosine-3′,5′-cyclic monophosphate (CPT), N6-benzoyladenosine-3′,5′-cyclic monophosphate (Bnz), 8-bromoadenosine-3′,5′-cyclic monophosphate, and its Rp counterpart (Rp-8-Br-cAMP) and the Epac-specific inhibitor ESI-09 were purchased from BioLog Life Science Institute (Bremen, Germany). The MEK inhibitor PD98059 (PD) was obtained from Calbiochem (Merck Chemicals, Nottingham, UK). Pertussis toxin from *Bordetella pertussis,* insulin, epidermal growth factor (EGF), hydrocortisone, (−)-adrenaline, (−)-noradrenaline, ISO, salbutamol, dobutamine, ICI-118,551, atenolol, H-89, forskolin, β-methyl-cyclodextrin, p-coumaric acid, and all other chemicals were obtained from Sigma-Aldrich (St. Louis, MO, USA). UK14304 was kindly provided by Pfizer (Sandwich, UK).

Cell culture and transfection

MCF-10A cells were obtained from American Type Culture Collection (ATCC; Manassas, VA, USA) and routinely grown in HEPES-buffered DMEM/Ham F12 culture medium containing antibiotics (100 μg/ml streptomycin, 100 IU/ml penicillin) and supplemented with 10% fetal calf serum (all from Invitrogen, Life Technologies, Rockville, MD. USA), 2 μg/ml insulin, 20 ng/ml EGF, and 0.1 μM hydrocortisone. Cells were subcultured once weekly by trypsinization (0.25% trypsin, 0.025% EDTA). For bioluminescence resonance energy transfer (BRET) experiments, MCF-10A cells were transiently transfected by electroporation with the indicated vectors (one 20 ms pulse at 1700 V) according to the manufacturer's procedures (Neon Transfection System MPK5000, Invitrogen) or using FuGENE (Promega, Madison, WI, USA). Then 4.5×10^5 transfected cells/well were plated onto 6-well plates, and BRET experiments were conducted 48 h post-transfection.

Measurement of cell proliferation

Cells were seeded in 6-well plates (3×10^5 cells/well) for cell counting or 96-well plates (5×10^3 cells/well) for DNA synthesis experiments, grown during 24 h in complete medium and then maintained for 18 h in growth factor/serum-free culture medium. Cell proliferation tests were then conducted in DMEM/Ham F12 medium supplemented with 2% charcoal-stripped fetal calf serum, 2 ng/ml EGF, 2 μg/ml insulin, and 0.1 μM hydrocortisone in the presence or absence of 0.1 μM ISO, which was changed every day. Proliferation response was evaluated at the indicated times by automatic cell counting (Beckman Coulter Z1 Cell-Counter, Beckman Coulter, Fullerton, CA, USA) or by methyl [^{3}H]-thymidine incorporation (0.4 μCi/well; DuPont NEN, Boston, MA, USA). After 6 or 24 h, cells were harvested in a Nunc Cell Harvester 8 (Nunc, Roskilde, Denmark), and radioactive nuclei retained into the glass fiber filters were counted in a liquid scintillation counter.

Measurement of Erk1/2 phosphorylation

Cells were seeded in 6-well plates (2.5×10^5 cells/well) and cultured over 24 h in complete medium. Cells were then growth factor/serum starved for 18 h. On the experiment day, cells were pretreated or not for 20 min with the indicated inhibitor and then stimulated or not for 20 min with the different agonists. Cells were then rapidly washed with ice-

cold PBS and lysed in RIPA buffer (10 mM Tris, pH 7.5; 150 mM NaCl; 2 mM Na ortho-vanadate; 0.1% SDS; 1% Igepal; and 1% Na deoxycholate). Equal amounts of proteins were separated on 10% SDS-PAGE and transferred to nitrocellulose membranes (Millipore, Billerica, MA, USA). Phosphorylated active Erk1/2 (p-Erk1/2) was detected using anti-p-Erk1/2 monoclonal antibody 1:1000 (sc-7383, Santa Cruz Biotechnology, Dallas, TX, USA). The membranes were stripped of IgG and reprobed with Erk2 (sc-154, Santa Cruz Biotechnology) or Erk1 (sc-94, Santa Cruz Biotechnology) polyclonal antibodies (1:2000) for protein loading normalization. Membranes were revealed by chemiluminescence using horseradish peroxidase–conjugated secondary antibody to anti-mouse or anti-rabbit IgG 1:10,000 (Amersham Biosciences GE Healthcare, Buc, France) and enhanced chemiluminescence detection solution (1.25 mM luminol, 0.2 mM *p*-coumaric acid, 0.06% v/v hydrogen peroxide, and 100 mM Tris-HCl, pH 8.8). Immunoblots were exposed to an autoradiographic film (Amersham Hyperfilm, GE Healthcare) and quantified by densitometry with ImageJ (U.S. National Institutes of Health, Bethesda, MD, USA). p-Erk1/2 was normalized according to protein load by expressing the data as a ratio of p-Erk1/2 over total Erk1 or Erk2 as indicated.

Immunofluorescence

Cells were seeded and cultured for 24 h in 6-well plates containing glass coverslips precoated with poly-L-lysine (1 mg/ml, Sigma-Aldrich) and then growth factor/serum starved for 18 h. On the day of the experiment, cells were treated or not for 15 min with the indicated compounds and then incubated during 15 min in Mg^{2+}/Ca^{2+}-free PBS. Cells were then washed, fixed with 4% paraformaldehyde in PBS for 10 min, permeabilized 15 min in blocking buffer (PBS, 0.3% Triton X-100, 0.2% BSA), and incubated 1 h at room temperature with anti-mouse β1-integrin antibody 1:1,000 (sc-9970, Santa Cruz Biotechnology). Immunoreactivity was revealed using a Texas Red conjugated secondary goat anti-mouse antibody 1:500 (Invitrogen, Molecular Probes). Cell nuclei were stained with 4′,6-diamidino-2-phenylindole 1:500 (Sigma-Aldrich) for 10 min. Visualization of fluorescence was monitored by an epifluorescence illuminating system, and digital images were captured using the AxioVision LE software (Carl Zeiss, Oberkochen, Germany).

Measurement of cell adhesion

Cells were seeded, in 6-wells plates (3×10^5 cells/well) for 48 h and pretreated or not for 20 min with the indicated inhibitors or antagonists and then exposed or not to the different ligands. The medium was removed, and the cells were incubated in Mg^{2+}/Ca^{2+}-free PBS containing 0.5 mM EDTA and 0.25% trypsin. After 15 min incubation at room temperature under constant shaking, detached cells were collected and counted (detached cells). Cells that resisted the treatment and remained adherent to the plastic were harvested following an additional 30 min incubation in Mg^{2+}/Ca^{2+}-free PBS containing 2.5 mM EDTA and 1.25% trypsin and counted (attached cells) using a cell counter. The percentage of adherent cells was calculated as follows: attached cells × 100/(attached cells+detached cells). This assay was validated by comparison with the method described by Bos *et al.* (16) and gave similar results.

Bioluminescence resonance energy transfer measurement

Encoding vectors for PKA subunits BRET probes RIα-Rluc8 and GFP2-Cα were previously described (32). GFP2-EPAC1-Rluc8 was obtained by subcloning EPAC1 coding sequence in pGFP2-MCS-Rluc8, obtained from Rluc8 subcloning in pGFP2-MCS-Rluc vector (Perkin Elmer, Wellesley, MA, USA). All generated constructs were confirmed by DNA sequencing. BRET constructs were transiently cotransfected into MCF-10A cells as indicated in the figure legends. At 48 h following transfection, cells were washed with PBS, detached with PBS/5 mM EDTA, and resuspended in PBS/0.1% (w/v) glucose at room temperature. Cells were then distributed in a 96-well microplate (Wallac, Perkin Elmer) and incubated in the presence or absence of forskolin and ISO for 30 min. $BRET^2$ between Rluc8 and GFP10/GFP2 was measured after the addition of the Rluc8 substrate coelenterazine 400a (5 μM; Interchim, Montulçon, France). $BRET^2$ readings were collected using a modified Infinite F500 (Tecan Group, Männedorf, Switzerland). The $BRET^2$ signal was calculated by the ratio of GFP2 (510–540 nm) emission over the light emitted by the Rluc8 (370–450 nm).

Total RNA extraction and real-time quantitative RT-PCR

Total RNA was extracted using RNeasy kit (Qiagen, Courtaboeuf, France). First-strand cDNA was synthesized using the SuperScriptII reverse transcriptase mix (Invitrogen). Negative controls without reverse transcriptase were performed to verify absence of contamination with genomic DNA. The primers used were from Applied Biosystems (Foster City, CA, USA): ADRB1: Hs00265096_s1; ADRB2: Hs00240532_s1 and ADRB3: Hs00609046_m1, 18S: Hs03928990_g1. Fluorogenic probe mix and the TaqMan Universal PCR Master Mix were Applied Biosystems. All amplification reactions were performed in duplicate from 20 ng cDNA using the Mx4000 Multiplex Quantitative PCR System (Stratagene, La Jolla, CA, USA) using the following conditions: 50°C for 2 min and 95°C for 10 min, followed by 40 cycles at 95°C for 15 s and 60°C for 1 min. Results were analyzed with Strategene MX4000 software. The threshold cycle C_t method (33) was used to calculate relative gene expression, and results were normalized to the C_t value of the housekeeping 18S gene.

Quantification of cAMP cell content

Total cAMP content was quantified using a competitive radio-binding assay for PKA using [^{3}H]-cAMP, as described previously (34). Briefly cells were seeded in 24-well plates (1.7×10^5 cells/well) in complete medium. After 24 h, medium was removed, and cells were incubated in RPMI medium without phenol red at 37°C for 10 min with different ISO concentrations and in the presence of 1 mM phosphodiesterase inhibitor 3-isobutyl-methylxantine. Stimulations were stopped by ethanol addition, and total cAMP was quantified. Cell extracts were centrifuged for 3 min at 3000 *g* at 4°C, and the recovered supernatant was evaporated and then resuspended in 50 mM Tris-HCl (pH 7.4) with 0.1% BSA for cAMP quantification.

Evaluation of PKA/Epac BRET probes distribution in light density membrane microdomains

Encoding vectors for PKA subunits BRET probes RIα-Rluc8 and GFP2-Cα or Epac1 BRET probe GFP2-EPAC1-Rluc8 were transiently transfected in MCF-10A cells as described for BRET experiments. At 48 h post-transfection, detergent-resistant membranes were obtained by sucrose flotation after solubilization of either whole cell. Briefly cells where solubilized in ice-cold lysis buffer (25 mM Tris, pH 7.4; 140 mM NaCl; 2 mM EDTA; and Roche protease inhibitor cocktail containing 1% v/v triton X-100). The resulting preparations

were loaded on a sucrose step gradient (5–40% discontinuous sucrose gradient). Sucrose solutions were prepared in the lysis buffer. Gradients were then centrifuged at 200,000 g for 18 h in an SW41 rotor (Beckman Optima L-100 XP Ultracentrifuge; Beckman Coulter). Twelve 1-ml fractions were collected from the top of the gradients. Each fraction was incubated in the presence of 5 μM coelenterazine H, and the total luminescence was measured using the Mithras LB 940 instrument (Berthold Technologies, Bad Wildbad, Germany). GM1 gangliosides were detected by dot-blot using peroxidase-coupled cholera toxin subunit B (Invitrogen).

Statistical analysis

Results are expressed as means ± SEM of ≥3 independent experiments as indicated. Statistical analysis was carried out using GraphPad Prism 4 software (GraphPad Software, San Diego, CA. USA). Statistical significance of the data was assessed using ANOVA followed by Dunnett's multiple test, Bonferroni or Tukey's test according to the design of the experiment. Unpaired Student's *t* test was used when comparing 2 groups. Values of $P < 0.05$ were considered statistically significant.

RESULTS

Femtomolar β-agonist concentrations promote MCF-10A cell adhesion

The effect of ISO, a nonselective β-agonist, was first tested on MCF-10A cell adhesion. For that purpose, we performed an adhesion assay by quantifying the percentage of cells remaining adherent to the plastic dishes following a specific cell detachment treatment as described in Materials and Methods. Here 0.1 μM ISO treatment resulted in a large and significant increase in the proportion of adhesive cells: 87.5 ± 6.3 *vs.* 35.0 ± 9.3% in control, $P < 0.0001$ (**Fig. 1*A***). The effect of the β-agonist on MCF-10A cell adhesion was further reinforced by immunofluorescence labeling of cell-matrix contacts using a β1-integrin antibody (Fig. 1*B*). Indeed, ISO treatment prevented cells from rounding and cell-matrix contact disruption since β1-integrin staining of the cells was markedly increased following detachment procedure when compared to control cells. ISO-promoted adhesion of MCF-10A cells was fast and robust, as the maximum of adhesion was reached almost immediately after 1 min of ISO treatment (82.6±5.3% of cells remaining adherent *vs.* 41±5.3% in control, $P<0.01$; Fig. 1*C*). It is noteworthy that, according to the low Hill slope value (0.248), the ISO dose-response curves were significantly better fitted using a 2-phase than a 1-phase model ($F=10.66$; $P<0.0001$) with an EC_{50} of 16.5 ± 11.5 fM for the first phase and an EC_{50} of 4.08 ± 3.09 nM for the second phase (Fig. 1*D*).

Nanomolar β-agonist concentrations inhibit MCF-10A cell proliferation through inhibition of Erk1/2 phosphorylation

The effect of ISO was next assessed on cell proliferation by evaluation of cell growth kinetics. Here 0.1 μM ISO resulted in a marked decrease in cell proliferation over time (**Fig. 2*A***). The inhibitory action of ISO on MCF-10A growth was significant after 24 h of treatment (16.3±2.1% reduction *vs.* control, $P<0.001$) and resulted in a 37.1 ± 3% ($P<0.001$ *vs.* control) reduction of cell growth after 48 h (Fig. 2*A*). These results were confirmed by quantification of DNA synthesis by a [^{3}H]-thymidine incorporation assay, which showed a

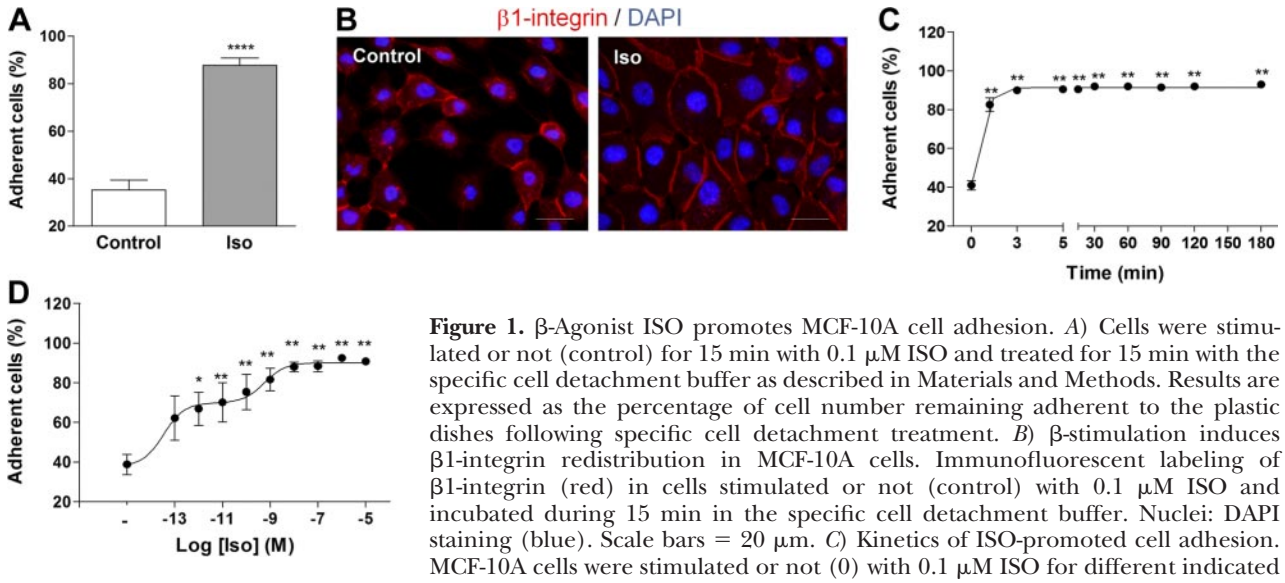

Figure 1. β-Agonist ISO promotes MCF-10A cell adhesion. *A*) Cells were stimulated or not (control) for 15 min with 0.1 μM ISO and treated for 15 min with the specific cell detachment buffer as described in Materials and Methods. Results are expressed as the percentage of cell number remaining adherent to the plastic dishes following specific cell detachment treatment. *B*) β-stimulation induces β1-integrin redistribution in MCF-10A cells. Immunofluorescent labeling of β1-integrin (red) in cells stimulated or not (control) with 0.1 μM ISO and incubated during 15 min in the specific cell detachment buffer. Nuclei: DAPI staining (blue). Scale bars = 20 μm. *C*) Kinetics of ISO-promoted cell adhesion. MCF-10A cells were stimulated or not (0) with 0.1 μM ISO for different indicated times, treated for 15 min with the specific cell detachment buffer, and then counted to determine cell adhesion percentage as in *A*. *D*) Effect of ISO on cell adhesion is concentration-dependent. Cells were stimulated or not (−) for 15 min with increasing concentrations of ISO, treated for 15 min with the specific cell detachment buffer and then counted to determine cell adhesion percentage as in *A*. Data represent means ± SEM of 4–6 independent experiments. Statistical significance was assessed using unpaired Student's *t* test (*A*) or ANOVA (*C, D*) followed by a Dunnett's test. *$P < 0.05$, **$P < 0.01$, ****$P < 0.0001$.

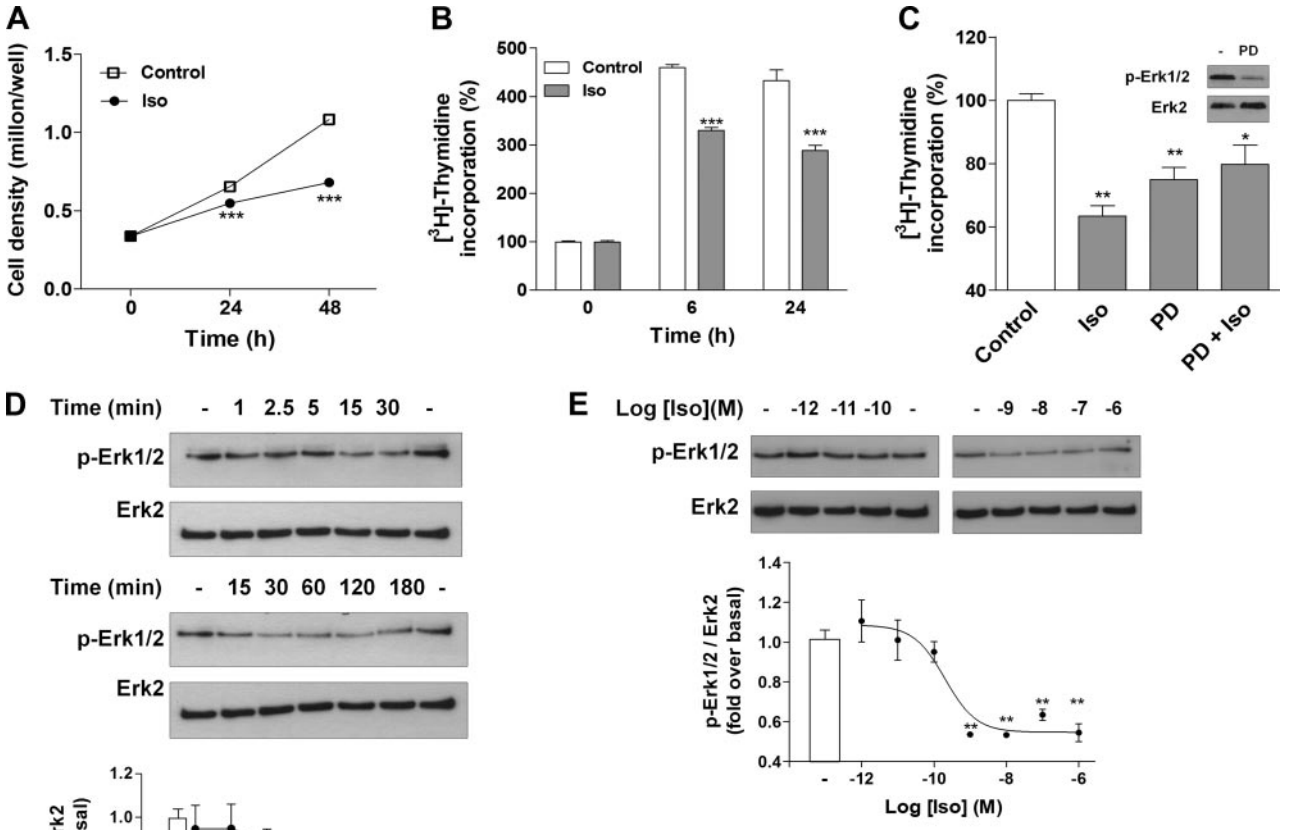

Figure 2. ISO inhibits MCF-10A cell proliferation through inhibition of Erk1/2 phosphorylation. *A*, *B*) Cells were stimulated or not (control) with 0.1 μM ISO for different times, and cell proliferation was evaluated by measurement of cell density (*A*) or DNA synthesis using [^{3}H]-thymidine incorporation (*B*) at each time point. Results are expressed as the percentage of control cells incubated in the absence of ISO (0). *C*) Cells were stimulated or not (control) with 0.1 μM ISO for 24 h in the presence or absence of 50 μM PD98059 (PD), and DNA synthesis was evaluated by [^{3}H]-thymidine incorporation. Inset: cells were treated or not with 50 μM PD for 15 min, and basal Erk1/2 phosphorylation (p-Erk1/2) was then measured by Western blot. *D*) Kinetics of ISO-mediated inhibition of p-Erk1/2. p-Erk1/2 was evaluated in cells stimulated or not (−) with 0.1 μM ISO for different indicated times. *E)* Dose responses of ISO-mediated inhibition of p-Erk1/2. MCF-10A cells were stimulated or not (−) with increasing concentrations of ISO for 20 min. Data represent means ± SEM of 3–7 independent experiments, performed in triplicates. Statistical significance was assessed using ANOVA followed by a Bonferroni (*A, B*) or Dunnett's test (*C–E*). $*P < 0.05$, $**P < 0.01$, $***P < 0.001$.

29.8 ± 2.1% ($P<0.001$ *vs.* control) significant reduction in [^{3}H]-thymidine incorporation following 6 h exposure to 0.1 μM ISO (Fig. 2*B*). This effect remained constant after 24 h ISO exposure (33.2±2.4% reduction *vs.* control, $P<0.001$). Given the central role of mitogen-activated protein kinases (MAPKs), and more specifically the Erk1/2 pathway in the regulation of cell proliferation, we examined the contribution of Erk1/2 to the proliferative effect of ISO. [^{3}H]-thymidine incorporation assays were conducted in the presence or not of PD, a specific and soluble MEK1 and 2 (Erk1/2 direct kinase effector) inhibitor. Cells were incubated for 24 h with 50 μM PD, a concentration that dramatically inhibited Erk1/2-phosphorylation in these cells (Fig. 2*C*, inset). PD significantly decreased [^{3}H]-thymidine incorporation by ~25.0 ± 10% ($P<0.01$; Fig. 2*C*), similarly to the inhibition observed in the presence of ISO (36.8±8% decrease when compared with control, $P<0.01$). However, costimulation of the cells with both ISO and PD did not further decrease [^{3}H]-thymidine incorporation detected for each individual compound (20±13%), thus indicating that ISO-mediated inhibition of MCF-10A cell proliferation by preventing Erk1/2 activation (Fig. 2*C*). Inhibition of Erk1/2-phosphorylation induced by 0.1 μM ISO was significant after 15 min stimulation and remained sustained over time at least until 200 min ($P<0.01$; Fig. 2*D*). Moreover, ISO significantly inhibited Erk1/2-phosphorylation according to a 1-site model with an EC_{50} of 0.25 ± 0.13 nM (Fig. 2*E*).

β_2-AR activation dually inhibits proliferation and promotes adhesion of MCF-10A cells

ISO is a nonspecific β-agonist targeting equally well all β-adrenergic receptor isoforms, thus preventing the identification of the β-AR subtype specifically involved in proliferation/adhesion of MCF-10A cells. Quantita-

tive RT-PCR performed on total mRNA extracted from MCF-10A revealed major expression of β_2-AR mRNA and, to a much lower extent, β_1-AR mRNA expression, while β_3-AR mRNA was undetectable (**Fig. 3*A***).

β-AR specificity of the inhibition of MCF-10A proliferation was assessed by measuring Erk1/2 phosphorylation following 20 min stimulation with different adrenergic agonists (Fig. 3*B*). Similarly to the inhibitory action of 0.1 μM ISO (68.0±9.0% decrease, $P<0.01$), a significant decrease of the basal Erk1/2-phosphorylation was also observed when cells were exposed to 0.1 μM natural catecholamines, epinephrine (Epi; 71.3±13% reduction *vs.* control, $P<0.01$), or norepinephrine (NE: 82±0.9% decrease, $P<0.01$). By contrast, 5 min exposure to 20 ng/ml EGF evoked a significant 98 ± 13% ($P<0.01$) increase in Erk1/2-phosphorylation while stimulation with 0.1 μM UK14,304 (UK), an α_2-adrenergic specific agonist, failed to modify basal Erk1/2-phosphorylation. To more accurately characterize the β-AR subtype responsible for the inhibition of cell proliferation, we conducted experiments using different β-subtype selective agonists and antagonists. Salbutamol (Salb), a specific β_2-AR agonist, induced a significant inhibition of Erk1/2-phosphorylation in the nanomolar range (EC_{50}: 0.31±0.16 nM; Fig. 3*C*), whereas the potency of the predominantly β_1-AR agonist dobutamine (Dob) in promoting inhibition was weaker (EC_{50}: 99.9±70 nM; Fig. 3*C*), thus indicating that the inhibition of Erk1/2-phosphorylation was primarily mediated by β_2-AR activation. In further support of this conclusion, similar experiments performed with β-antagonists showed that ICI-118,551 (ICI), a β_2-AR selective antagonist, was able to block the Epi-mediated inhibition of Erk1/2-phosphorylation in MCF-10A cells at concentrations as low as 10 nM, while atenolol, a β_1-selective antagonist, had no effect over a wide range of concentrations (Fig. 3*D*).

Similarly, we determined the β-AR subtype involved in the stimulation of MCF-10A cell adhesion. Endogenous catecholamines Epi and NE but also ISO (0.1 μM) all induced a significant increase in cell adhesion (Epi: 87±7.5%; NE: 71±9.7%; ISO 87.7±6.34% *vs.* control 35.2±9.36%, $P<0.01$), while UK did not have any effect on cell adhesion (Fig. 3*E*). More selective β_2-agonists,

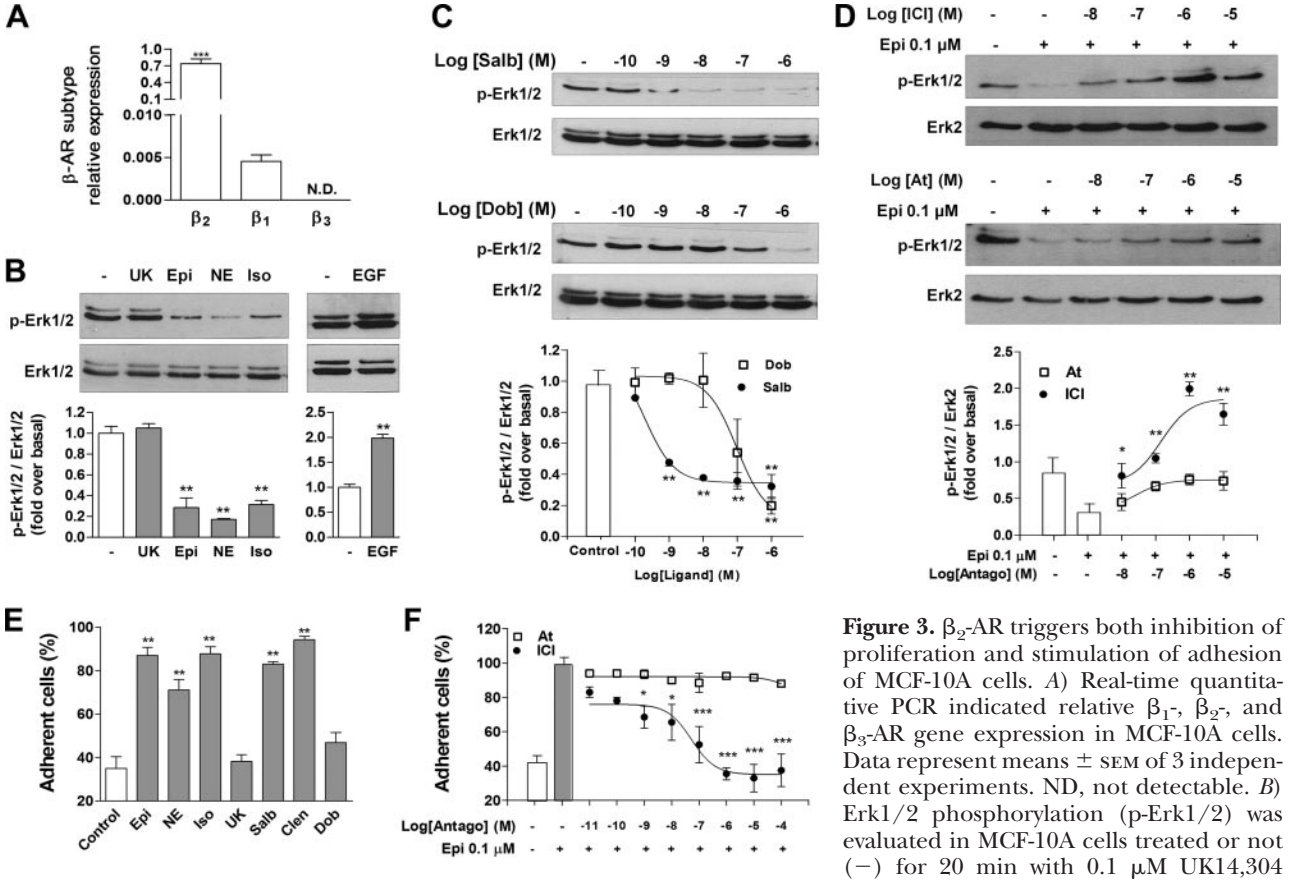

Figure 3. β_2-AR triggers both inhibition of proliferation and stimulation of adhesion of MCF-10A cells. *A*) Real-time quantitative PCR indicated relative β_1-, β_2-, and β_3-AR gene expression in MCF-10A cells. Data represent means ± SEM of 3 independent experiments. ND, not detectable. *B*) Erk1/2 phosphorylation (p-Erk1/2) was evaluated in MCF-10A cells treated or not (−) for 20 min with 0.1 μM UK14,304 (UK), epinephrine (Epi), norepinephrine (NE), or isoproterenol (ISO). Stimulation for 5 min with 20 ng/ml EGF was used as a positive control. *C*) p-Erk1/2 was evaluated in cells treated or not (−) for 20 min with increasing concentrations of β_2-agonist salbutamol (Salb) or β_1-agonist dobutamine (Dob). *D*) p-Erk1/2 was evaluated in MCF-10A cells treated or not (−) for 20 min with 0.1 μM Epi in the presence or not (−) of increasing concentrations β-antagonists ICI-118,551 (ICI) or atenolol (At). *E*) Cell adhesion was evaluated as in Fig. 1 in MCF-10A cells treated or not (control) for 15 min with 0.1 μM Epi, NE, ISO, UK, or 10 nM Salb, clenbuterol (Clen), and Dob. *F*) Cell adhesion was evaluated in cells treated or not for 15 min with 0.1 μM Epi in the presence or not (−) of increasing concentrations β-antagonists ICI or At. Data represent means ± SEM of 3 to 4 independent experiments performed in triplicate. Statistical significance was assessed using an unpaired *t* test (*A*) or ANOVA followed by a Dunnett's test (*B–F*). For panels *D* and *F*, comparison group was Epi 0.1 μM. $*P < 0.05$, $**P < 0.01$, $***P < 0.001$.

Salb and clenbuterol, also evoked a significant increase in cell adhesion at 10 nM, while 10 nM Dob failed to induce cell adhesion. Moreover, only the β_2-specific antagonist ICI was able to dose dependently inhibit the Epi-induced cell adhesion (Fig. 3*F*), thus demonstrating that adrenergic activation of MCF-10A cell adhesion is also controlled by the β_2-AR subtype.

β_2-AR regulates MCF-10A cell proliferation and adhesion through two distinct cAMP pathways

β_2-AR dually couples to both G_s and G_i proteins to regulate adenylyl cyclase (AC), but can also signal *via* G protein-independent pathways (35). To investigate the molecular mechanisms whereby β_2-AR decreases proliferation but increases adhesion of MCF-10A cells, we first assessed the implication of the G-protein/cAMP pathway. Interestingly, stimulation with 10 μM forskolin induced a significant reduction of basal Erk1/2-phosphorylation (**Fig. 4*A***) while significantly promoting cell adhesion comparable to that observed in the presence of ISO (Fig. 4*B*). Similar results were obtained when cells were stimulated with 100 μM 8-Br-cAMP (8-Br), a permeable analog of the natural cAMP (Fig. 4*A, B*). Pretreatment with 100 ng/ml pertussis toxin (PTX) for 16 h did not modify either Erk1/2-phosphorylation inhibition or adhesion activation mediated by β_2-AR activation (Fig. 4*C, D*), while it completely prevented the inhibitory effect of UK on forskolin-mediated Erk1/2-phosphorylation inhibition (Fig. 4*C*, right panel), suggesting that the regulation of β_2-AR-dependent proliferation and adhesion is not a consequence of receptor coupling to G_i, but rather depends on the classical activation of a G_s AC/cAMP pathway.

To get further insight into the cAMP downstream effectors involved in proliferation inhibition and cell adhesion stimulation, we next assessed the implication of PKA and Epac, the two cAMP direct effectors (2). For that purpose, we tested pharmacological inhibitors/activators exhibiting specificity toward PKA or Epac: H-89 is a specific PKA inhibitor; Bnz is a potent general activator of PKA with poor Epac efficacy; Rp-8-Br-cAMP (Rp) is a competitive inhibitor of cAMP binding to PKA discriminating between the two PKA isoforms and exhibiting more PKAI selectivity (36); the CPT is a potent stimulator of Epac and an extremely poor PKA activator; ESI-09 is a new inhibitor of both Epac1 and Epac2, displaying 100-fold selectivity for Epac proteins compared to PKA (37). As shown in Fig. 4*E*, the inhibition of Erk1/2-phosphorylation mediated by ISO was mimicked by stimulation with 100 μM Bnz but not by 100 μM CPT, most likely indicating that inhibition of cell proliferation occurred through PKA activation. These results were confirmed by the use of 100 μM Rp or 50 μM H-89 (Fig. 4*E*) which completely prevented ISO-dependent inhibition of Erk1/2 activation, while 50 μM ESI-09 had no effect (Fig. 4*E*). On the contrary, only CPT and not Bnz was able to mimic ISO-mediated stimulation of cell adhesion (Fig. 4*F*), while 50 μM ESI-09 (but not H-89 or Rp) pretreatment was highly effective at inhibition of cell adhesion induced by different ISO concentrations (Fig. 4*F*), thus strongly supporting that ISO promotes cell adhesion through an Epac-dependent pathway. All these results demonstrating the specific roles of PKA and Epac in cell proliferation and cell adhesion respectively were confirmed by complementary molecular/genetic approaches competing with endogenous PKA or Epac proteins by transiently overexpressing a PKA inhibitor (PKI; ref. 38) or an Epac-dominant negative (N-Epac; ref. 39). Indeed, specific inhibition of PKA by PKI overexpression did not modify ISO-induced cell adhesion but completely prevented ISO-mediated inhibition of Erk1/2 phosphorylation (Supplemental Fig. S1*A*). Conversely, overexpression of N-Epac did not affect ISO-mediated p-Erk1/2, while it significantly decreased cell adhesion induced by ISO by 21.1 ± 3.1% (Supplemental Fig. S1*B*). Finally, cell adhesion promoted by ISO-dependent cAMP production was completely independent from Erk1/2-phosphorylation, since it was completely insensitive to PD (Fig. 4*G*).

Altogether these results demonstrate that ISO triggers both inhibition of Erk1/2-phosphorylation (proliferation) and activation of cell adhesion through stimulation of the same β_2-AR receptor but using distinct pathways, both dependent on cAMP production. While the inhibition of Erk1/2-phosphorylation depends on PKA activation, conversely, the increase in cell adhesion relies on an Epac-dependent mechanism. Interestingly, while both PKA and Epac are both cAMP effectors, we were unable to depict fentomolar cAMP production promoted by ISO in MCF-10A cells (Fig. 4*H*) and contrary to ISO-induced cell adhesion (Fig. 1*D*), ISO-cAMP dose-response curves were fitted to a 1-site model with an EC_{50} of 200.3 ± 9.6 nM (Fig. 4*H*).

β_2-AR regulates cell proliferation and adhesion through two distinct compartmentalized receptor populations

Because ISO was regulating MCF-10A cell proliferation and adhesion through distinct cAMP-dependent pathways, we next evaluated if these effects could rely on activation of different β_2-AR populations distributed along distinct plasma membrane microdomains. More specifically, we assessed the compartmentalization into cholesterol-enriched raft membrane domains, which classically concentrate specific receptor/effectors and direct specific cellular signaling when compared to nonraft domains (40). For that purpose we took advantage of the use of the pharmacological β-methyl-cyclodextrin (βCD), a specific scavenger that extracts cholesterol from the plasma membrane, thus downregulating the presence of raft microdomains. A previous report described that pretreatment of MCF-10A cells with 5 mM βCD promoted ~50% cholesterol depletion in these cells (41). Pretreatment of MCF-10A cells with different βCD concentrations up to 5 mM caused a significant dose-response inhibition of ISO-promoted cell adhesion with no significant modifica-

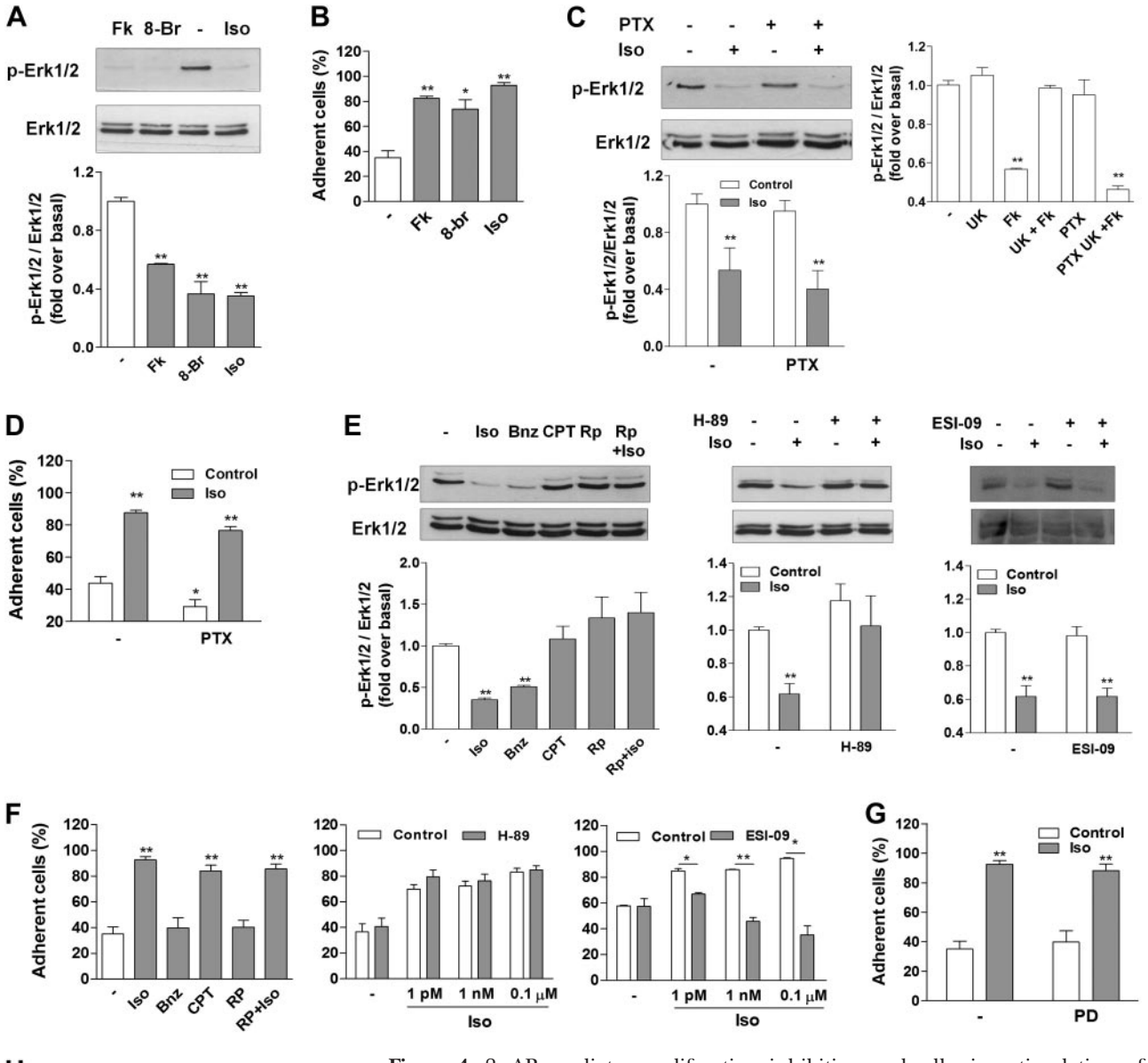

Figure 4. β_2-AR mediates proliferation inhibition and adhesion stimulation of MCF-10A cells through PKA and Epac respectively. *A*, *B*, *E*, *F*) MCF-10A cells were stimulated or not (−) with 0.1 μM ISO, 10 μM forskolin (Fk), 100 μM cAMP analogs: 8-Br-cAMP (8-Br), Bnz, CPT, or Rp-8-Br-cAMP (Rp), in the presence or not of 50 μM H-89 PKA inhibitor or ESI-09 Epac inhibitor during 20 min for the evaluation of Erk1/2 phosphorylation (p-Erk1/2) (*A, E*) or 15 min for cell adhesion (*B, F*). *C, D*) MCF-10A cells were pretreated or not (−) 16 h with 100 ng/ml pertussis toxin (PTX) and stimulated or not (control) with 0.1 μM ISO during 20 min for the evaluation of p-Erk1/2 inhibition (*C*) or 15 min for cell adhesion (*D*). As a positive control for PTX, cells were stimulated or not with 0.1 μM UK14,304 (UK) or 10 μM Fk or both during 20 min and pretreated or not with PTX for the evaluation of p-Erk1/2 inhibition (*C*, right panel). *G*) MCF-10A cells were pretreated or not (−) for 15 min with 50 μM MEK1/2 inhibitor PD98059 (PD) and stimulated or not (control) with 0.1 μM ISO during 15 min for the evaluation of cell adhesion. *H*) Total cAMP content was measured in MCF-10A cells following 10 min stimulation with increasing ISO concentrations. Cell adhesion was evaluated as in Fig. 1. Data represent means ± SEM of 3 or 4 independent experiments performed in triplicate. Statistical significance was assessed using ANOVA followed by a Dunnett's test (*A–E, G, H*) or Bonferroni test (*F*). $*P < 0.05$, $**P < 0.01$.

tion of basal cell adhesion (**Fig. 5*A***). Interestingly, similar βCD treatments had no effect on the inhibition of Erk1/2-phosphorylation mediated by ISO (Fig. 5*B*). Thus, these results most likely indicate that ISO promotes MCF-10A cell adhesion by activating a β_2-AR localized into specific raft microdomains, while it inhibits Erk1/2-phosphorylation through activation of another β_2-AR present in nonraft domains. These conclusions were reinforced by bioluminescence resonance energy transfer ($BRET^2$) experiments to directly assess

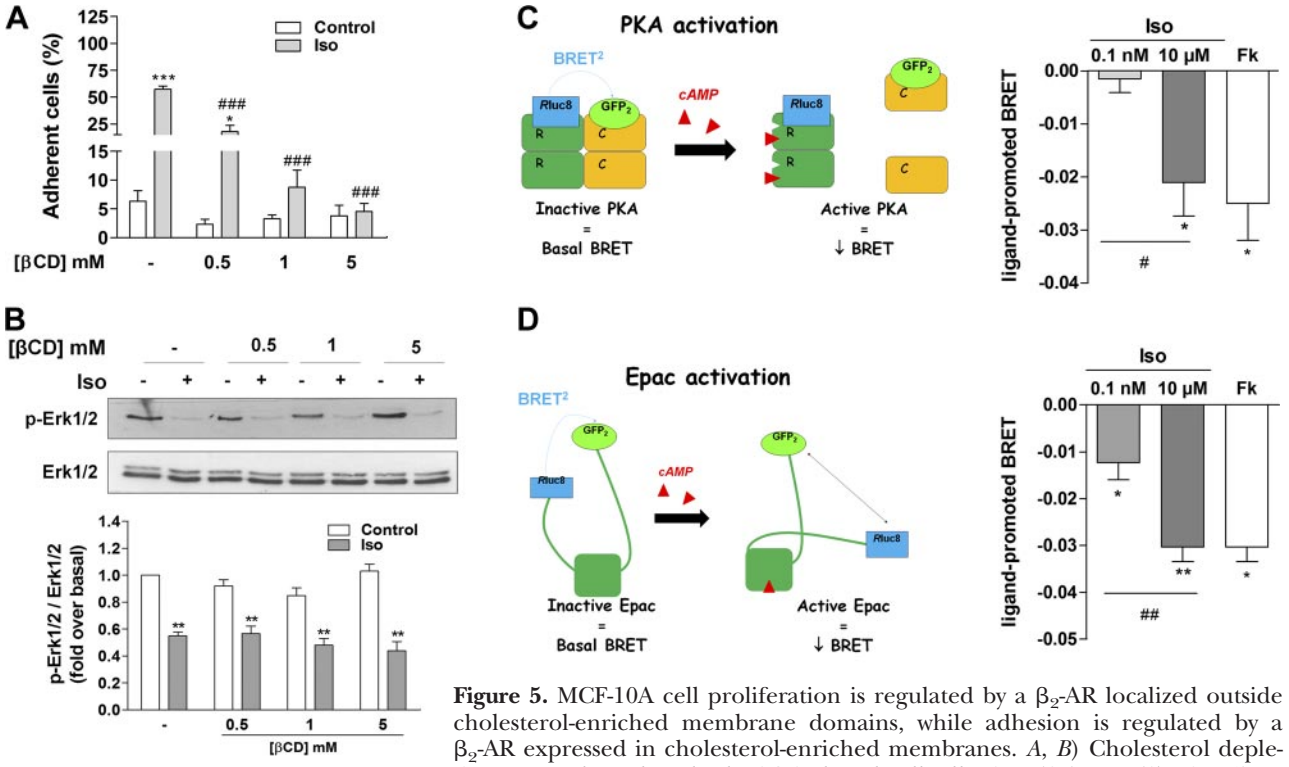

Figure 5. MCF-10A cell proliferation is regulated by a β_2-AR localized outside cholesterol-enriched membrane domains, while adhesion is regulated by a β_2-AR expressed in cholesterol-enriched membranes. *A*, *B*) Cholesterol depletion was evaluated on both ISO-induced cell adhesion (0.1 μM, 15 min; *A*) or ISO-induced inhibition of Erk1/2 phosphorylation (p-Erk1/2; 0.1 μM, 20 min; *B*) in MCF-10A cells pretreated or not (−) with increasing concentrations β-methyl-cyclodextrin (βCD). *C*, *D*) PKA or Epac activation was evaluated in real time in MCF-10A cells transiently expressing respectively BRET biosensors RIα-Rluc8 and GFP2-Cα (*C*) or GFP2-EPAC1-Rluc8 (*D*). BRET signals were recorded as described in Materials and Methods following stimulation or not (basal) of MCF-10A cells with 0.1 nM or 10 μM of ISO or 10 μM forskolin (Fk). Results are expressed as the difference in the BRET signal measured in the presence and the absence of agonist. Left panels show representative illustration of PKA or Epac biosensors principle. Data represent means ± SEM of 3–5 independent experiments. Statistical significance was assessed using ANOVA followed by a Tukey's test. $^{*}P < 0.05$, $^{**}P < 0.01$, $^{***}P < 0.001$ between stimulated and nonstimulated cells (control); $^{\#}P < 0.05$, $^{\#\#}P < 0.01$, $^{\#\#\#}P < 0.001$ between the different βCD (*A*) or the 2 ISO concentrations (*C*, *D*).

the activation of PKA and Epac by β_2-AR in MCF-10A cells. The activation of both PKA and Epac1 BRET biosensors by cAMP is reflected by a decrease in the BRET signal, correlating with PKA regulator subunit dissociation from the catalytic subunit (32) or a conformational change in Epac1. Thus, when MCF-10A cells were transiently transfected with PKAI or Epac1 BRET biosensors, 10 μM forskolin stimulation promoted a significant BRET decrease for both biosensors, validating the cAMP-dependent activation of both effectors in these cells (Fig. 5*C*, *D*). Interestingly, PKA biosensor activation only occurred at high ISO concentrations, as indicated by the significant decrease of the BRET signal in the presence of 10 μM ISO but not 0.1 nM (Fig. 5*C*). In contrast, Epac1 was dose dependently activated at both low and high ISO concentrations (0.1 nM and 10 μM), as reflected by the gradual decrease in the BRET signal (Fig. 5*D*). Specific ISO responses toward PKA and Epac probes did not relate to specific and different localization of the two probes since they distributed similarly inside and outside cholesterol-enriched domains in sucrose gradients following cell solubilization with 1% Triton-X100 (Supplemental Fig. S2). These results corroborate our previous findings and support the idea that low ISO concentrations promote cell adhesion only *via* Epac activation in lipids rafts, while high ISO concentrations engage another additional cell proliferation inhibition mediated by PKA and not by Epac in non-cholesterol-enriched domains (**Fig. 6**).

DISCUSSION

The results presented in this paper unveil important molecular mechanisms through which the β_2-AR couples with the cAMP signaling machinery as a function of agonist dose.

One major finding of our study is that β_2-AR coordinates both stimulation of adhesion and inhibition of proliferation of nontumor breast MCF-10A cells using a dose-dependent but dual cAMP-based signaling mechanism. Indeed, we found that low β-agonist concentrations trigger cell adhesion exclusively through a cAMP/Epac-dependent pathway, whereas higher concentrations engage an additional cAMP module using PKA as effector and mediating the inhibition of Erk1/2-dependent cell proliferation (Fig. 6). This original dose-dependent regulation of β_2-AR signaling has previously been reported for the MAPK Erk1/2 activation in MEF cells, in which a G-protein-dependent and another G

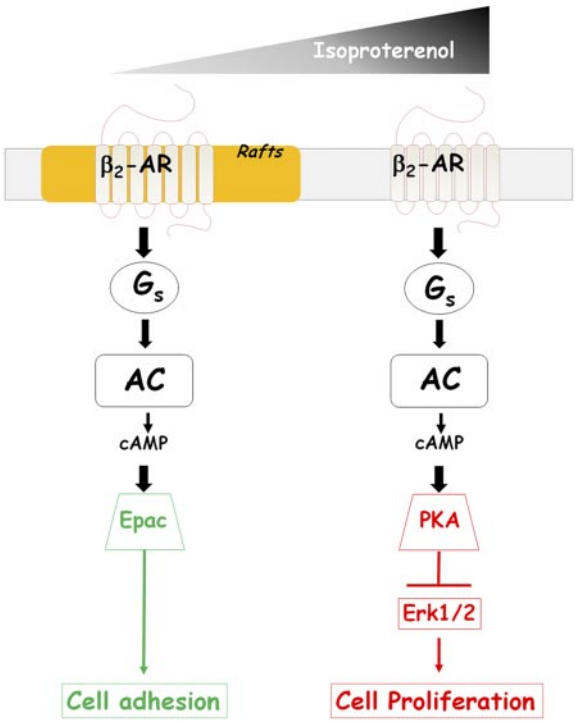

Figure 6. Schematic representation of β_2-AR-dependent cAMP signaling coordinating adhesion and proliferation of MCF-10A cells. Low-concentration β-agonist ISO trigger cell adhesion only through a β_2-AR/cAMP/Epac-dependent pathway compartmentalized in cholesterol-enriched rafts microdomains. Increasing ISO concentrations engage an additional cAMP module using PKA as cAMP transmitter and controlled by another β_2-AR localized in nonraft domains, which mediates the inhibition of MCF-10A cell Erk1/2-dependent proliferation.

protein-independent, but Src-dependent, mechanism were identified for low and high agonist concentrations, respectively (42). The researchers speculated that low agonist concentrations favored the engagement of the G protein to the receptor in agreement with high affinity agonist binding, while higher concentrations should lead to activation of a non-G-protein signaling. This hypothesis could not be reconciled with our results, since we showed that both agonist-dependent phases required cAMP production most probably through direct G_s activation. Moreover, and similarly to the study of Sun *et al.* (42), we found that the signaling pathways involved in the effects of high agonist concentrations resulted from the addition of PKA activation to the Epac activation observed at low concentrations, thus precluding the existence of a dose-dependent switch mechanism as originally suggested. It remains unclear how β_2-AR can indeed elicits two different signaling outputs when binding a single ligand. In the presence of high agonist concentrations, purified β_2-AR has been shown to exist in two distinct active biophysical conformations (43), which could underlie the two different β_2-AR signaling outputs observed at high and low ISO concentrations. In this regard, an interesting point of our study is that we demonstrated that the cAMP/Epac/adhesion signaling module was β-cyclodextrin sensitive while the cAMP/PKA/proliferation one was not, strongly suggesting that both effects most likely rely on the existence of two β_2-AR populations localized in two distinct plasma membrane microdomains. The β_2-AR adhesion signaling platform would be concentrated in cholesterol-enriched domains while that mediating the β_2-AR-dependent antiproliferative effect would reside outside. These results are similar to those for the oxytocin receptor, another GPCR, for which promotion of cell growth inhibition would be taking place outside rafts/caveolin-rich domains (44), while cell adhesion most likely requires specific β-integrin adhesion proteins concentrated in lipid raft domains in agreement with raft-regulating β-integrin activity (45). In this context, one possible explanation for two different cAMP pathways engaged by β_2-AR activation could rely on the existence of two structurally different receptor conformations stabilized by the agonist, depending on its localization inside or outside cholesterol-enriched raft membrane domains. Consistent with this hypothesis, a recent study reported that cholesterol alters the structural properties of β_2-AR (46) and that this could in part influence β_2-AR ligand binding response. Moreover, the presence of two different pools of β_2-ARs, both inside and outside rafts in MCF-10A cells, is not aberrant since this receptor was already localized inside (47) or outside (48) lipid rafts, depending on the cell type. Numerous examples of GPCR localization determining signaling output are now available in the literature (40) and could easily reconcile the fact that β_2-ARs concentrated in lipid rafts control cell adhesion while the β_2-ARs localized in nonraft domains inhibit cell proliferation.

The second interesting observation in our study is the capacity of the β_2-AR to simultaneously couple to dual AC/cAMP signaling modules, 1 impacting on Epac activation and another on PKA, to regulate two individual signaling outcomes. Since both PKA and Epac, the two main cAMP effectors, are ubiquitously expressed in all cells, it is not surprising that increasing intracellular cAMP levels nonspecifically leads to the concomitant activation of both effectors. However, the existence of two highly coordinated cAMP effectors controlled by specific receptor activation argues for a spatiotemporal control of the cAMP signaling pathways initiated in a cell. Studies in this field have shown that GPCR activation can select one of the two cAMP effectors, thus favoring PKA or Epac activation depending on the cellular context (28, 49). PKA and Epac can act antagonistically (50, 51), but concomitant activation of both effectors by the same receptor has also been reported to synergize the regulation of a common downstream effector (52, 53). To our knowledge, the identification of a single receptor mediating both Epac and PKA activation leading to different signaling outcomes has not been reported previously. Compartmentalized cAMP signaling within specific spatially sequestered receptor-AC-PKA/Epac–PDE modules in rafts and nonraft domains most probably accounted for this cAMP output diversity (54, 55). In line with this as-

sumption, β_1-AR, able to promote both PKA and Epac activation in adult cardiomyocytes, was shown to exist as two subpopulations localized in lipid rafts and nonraft domains, and only the β_1-AR localized inside rafts was able to elicit PKA activation (56). Indeed, segregation of different and specific β_2-AR/cAMP signaling modules expressed in discrete parts of the plasma membrane could relate to a number of factors: coupling of β_2-AR with specific AC isoforms; localization of specific ACs in defined structural membrane domains; sequestration of Epac/PKA by specific A-kinase anchoring proteins (AKAPs; ref. 55; >70 different AKAP isoforms have been identified so far, ref. 57, and they have been shown to sequester highly diverse proteins, such as GPCRs, ACs, PDEs, PKAs, and Epac); and selective anchorage of PDEs, enzymes that degrade cAMP, to distinct intracellular sites (55). It follows that the equilibrium between these different proteins could pattern the cAMP response as recently highlighted (58). Until now, segregated cAMP signaling at the plasma membrane has been only depicted through the use of FRET-based biosensor imaging, allowing real-time and spatial resolution of cAMP local production in a single cell (59). Thus, classical other approaches measuring total cAMP production with poor spatiotemporal resolution most probably miss cAMP production in discrete cell compartments. Accordingly, in our study, femtomolar activation of cAMP/Epac/adhesion signaling module by ISO could not be picked out from global cAMP measurements. Another intriguing finding of our study is the biphasic activation MCF-10A cells adhesion promoted by ISO, with both phases associated with cAMP/Epac signaling localized in cholesterol-enriched domains. While our study did not dissect this phenomenon, several explanations could be inferred, such as the activation of 2 Epac isoforms (Epac1 and Epac2) by β_2-AR to coordinate cell adhesion, each of them potentially compartmentalized in different rafts domains (caveolae *vs.* noncaveolae rafts).

To our knowledge, little is known about β-adrenergic action in noncancer breast cells. Here we demonstrate that β_2-AR stimulation of MCF-10A cells promotes a rapid increase in cell adhesion and an additional inhibition of cell proliferation. This result is consistent with a previous report, describing that, in the same cells, β-AR stimulation promotes lumen formation in 3-dimensional cultures as a reflection of cell differentiation, a process known to require cell growth inhibition (5). Predominant β_2-AR subtype expression was also evidenced in mammary glands from different species (60, 61). The cAMP-dependent inhibitory action of β_2-adrenergic agonists on cell proliferation observed in MCF-10A cells is consistent with previous *in vitro* and *in vivo* studies in different breast cancer cell lines. Pirbuterol (a β_2-AR agonist) inhibits the growth of human breast cancer cells *in vivo* by blocking the Raf-1/Erk1/2 pathway *via* a cAMP/PKA-dependent mechanism (28). ISO suppresses the growth of MDA-MB-231 human breast cancer cells through increased cAMP production, and this effect is blocked by propranolol and mimicked by 8-Br-cAMP (21). In addition, we have previously demonstrated that in several breast cancer cell lines, the activation of endogenous β_2-AR is associated with a decrease in cell proliferation. This effect is mimicked by cAMP analogs and is PKA dependent (23).

In this study, we found exclusive actions for both PKA and Epac, since Epac was promoting cell adhesion while PKA was specifically controlling the inhibition of MCF-10A cell growth. Bos *et al.* (62) supported a model in which PKA can directly phosphorylate and inactivate Raf1, leading to Erk1/2 pathway inhibition. In contrast, and consistent with the Epac-independent Erk1/2 inhibition observed in our study, Epac usually mediates the activation of Rap1 and is not directly involved in the regulation of the Raf1/B-Raf-Erk pathway (62, 63). Pharmacological manipulation of both Epac and PKA allowed us to determine the specific involvement of Epac in β_2-AR agonist-induced cell adhesion through a PKA-independent mechanism. Similar results were obtained in an ovarian cancer cell line, where β_2-adrenergic stimulation induced integrin-mediated cell adhesion to fibronectin *via* cAMP production and Epac and Rap1 activation (16).

In sumary, the β_2-AR reveals an intricate mode of cAMP signaling to coordinate control of both cell adhesion and proliferation. During the last few years, control of cellular signaling through the existence of compartmentalized modules has emerged as a fundamental mechanism allowing spatiotemporal regulation. Now deciphering the molecular mechanisms that underlay the different signaling modules remains a challenge in order to provide specific targeting of the desired cell behavior. In this study we provide new insights into β_2-AR-cAMP-signaling pathways governing adhesion/proliferation of the nontumor human breast cell line MCF-10A, which in turn could have a major impact in the field of cancer. The signaling mechanisms involved in cell adhesion and proliferation in these cells are a matter of great interest because they are key processes deregulated during tumor progression. FJ

This paper is dedicated to the memory of the authors' friend and colleague Dr. Hervé Paris, who was the mentor of this work and passed away suddenly during its completion. This work was supported by a grant from the Ministerio de Ciencia, Tecnología e Innovación Productiva (MINCyT)/EcosSud Argentina/Francia, Proyecto de Investigación en Ciencia y Tecnología (PICT) 2011#103 Agencia Nacional de Promoción Científica y Tecnológica (ANPCyT) and Proyecto de Investigación Plurianual (PIP 2010–2012#692–Consejo Nacional de Investigaciones Cientificas y Tecnicas (CONICET), and Fundación Roemmers. A.B. was a recipient of an Oster fellowship from Fundación Bunge y Born Argentina. The authors especially thank Sabrina Copsel, Lucía Gargiulo, Carlos Davio, Lauriane Onfroy, Colette Denis, and Marie-Hélène Seguelas for their invaluable technical help, Silvio Gutkind (U.S. National Institutes of Health/National Institute of Dental and Craniofacial Research, Bethesda, MD, USA) and Omar Coso [Facultad de Ciencias Exactas y Naturales (FCEN)–Instituto de Fisiologíca, Biología Molecular y Neurociencias (IFIBYNE), Universidad de Buenos

Aires–CONICET, Buenos Aires, Argentina] for generously providing PKI and N-Epac encoding vectors, and Lucrecia Calvo for critical reading of the manuscript.

REFERENCES

1. Daly, C. J., and McGrath, J. C. (2011) Previously unsuspected widespread cellular and tissue distribution of beta-adrenoceptors and its relevance to drug action. *Trends Pharmacol. Sci.* **32,** 219–226
2. Cheng, X., Ji, Z., Tsalkova, T., and Mei, F. (2008) Epac and PKA: a tale of two intracellular cAMP receptors. *Acta Biochim. Biophys. Sin.* **40,** 651–662
3. Kim, M. O., Lee, Y. J., Park, J. H., Ryu, J. M., Yun, S. P., and Han, H. J. (2012) PKA and cAMP stimulate proliferation of mouse embryonic stem cells by elevating GLUT1 expression mediated by the NF-kappaB and CREB/CBP signaling pathways. *Biochim. Biophys. Acta* **1820,** 1636–1646
4. Toll, L., Jimenez, L., Waleh, N., Jozwiak, K., Woo, A. Y., Xiao, R. P., Bernier, M., and Wainer, I. W. (2011) β2-adrenergic receptor agonists inhibit the proliferation of 1321N1 astrocytoma cells. *J. Pharmacol. Exp. Ther.* **336,** 524–532
5. Nedvetsky, P. I., Kwon, S. H., Debnath, J., and Mostov, K. E. (2012) Cyclic AMP regulates formation of mammary epithelial acini in vitro. *Mol. Biol. Cell* **23,** 2973–2981
6. Li, D. M., and Feng, Y. M. (2011) Signaling mechanism of cell adhesion molecules in breast cancer metastasis: potential therapeutic targets. *Breast Cancer Res. Treat.* **128,** 7–21
7. Chen, L., Zhang, J. J., and Huang, X. Y. (2008) cAMP inhibits cell migration by interfering with Rac-induced lamellipodium formation. *J. Biol. Chem.* **283,** 13799–13805
8. Grandoch, M., Rose, A., ter Braak, M., Jendrossek, V., Rubben, H., Fischer, J. W., Schmidt, M., and Weber, A. A. (2009) Epac inhibits migration and proliferation of human prostate carcinoma cells. *Br. J. Cancer* **101,** 2038–2042
9. Mantovani, G., Lania, A. G., Bondioni, S., Peverelli, E., Pedroni, C., Ferrero, S., Pellegrini, C., Vicentini, L., Arnaldi, G., Bosari, S., Beck-Peccoz, P., and Spada, A. (2008) Different expression of protein kinase A (PKA) regulatory subunits in cortisol-secreting adrenocortical tumors: relationship with cell proliferation. *Exp. Cell Res.* **314,** 123–130
10. Rivas, M., and Santisteban, P. (2003) TSH-activated signaling pathways in thyroid tumorigenesis. *Mol. Cell. Endocrinol.* **213,** 31–45
11. Thaker, P. H., Han, L. Y., Kamat, A. A., Arevalo, J. M., Takahashi, R., Lu, C., Jennings, N. B., Armaiz-Pena, G., Bankson, J. A., Ravoori, M., Merritt, W. M., Lin, Y. G., Mangala, L. S., Kim, T. J., Coleman, R. L., Landen, C. N., Li, Y., Felix, E., Sanguino, A. M., Newman, R. A., Lloyd, M., Gershenson, D. M., Kundra, V., Lopez-Berestein, G., Lutgendorf, S. K., Cole, S. W., and Sood, A. K. (2006) Chronic stress promotes tumor growth and angiogenesis in a mouse model of ovarian carcinoma. *Nat. Med.* **12,** 939–944
12. Armaiz-Pena, G. N., Allen, J. K., Cruz, A., Stone, R. L., Nick, A. M., Lin, Y. G., Han, L. Y., Mangala, L. S., Villares, G. J., Vivas-Mejia, P., Rodriguez-Aguayo, C., Nagaraja, A. S., Gharpure, K. M., Wu, Z., English, R. D., Soman, K. V., Shazhad, M. M., Zigler, M., Deavers, M. T., Zien, A., Soldatos, T. G., Jackson, D. B., Wiktorowicz, J. E., Torres-Lugo, M., Young, T., De Geest, K., Gallick, G. E., Bar-Eli, M., Lopez-Berestein, G., Cole, S. W., Lopez, G. E., Lutgendorf, S. K., and Sood, A. K. (2013) Src activation by beta-adrenoreceptors is a key switch for tumour metastasis. *Nat. Commun.* **4,** 1403
13. Tagliaferri, P., Katsaros, D., Clair, T., Ally, S., Tortora, G., Neckers, L., Rubalcava, B., Parandoosh, Z., Chang, Y. A., Revankar, G. R., Crabtree, G. W., Robins, R. K., and Cho-Chung, Y. S.. (1988) Synergistic inhibition of growth of breast and colon human cancer cell lines by site-selective cyclic AMP analogues. *Cancer Res.* **48,** 1642–1650
14. Tagliaferri, P., Katsaros, D., Clair, T., Neckers, L., Robins, R. K., and Cho-Chung, Y. S. (1988) Reverse transformation of Harvey murine sarcoma virus-transformed NIH/3T3 cells by site-selective cyclic AMP analogs. *J. Biol. Chem.* **263,** 409–416
15. Tortora, G., Tagliaferri, P., Clair, T., Colamonici, O., Neckers, L. M., Robins, R. K., and Cho-Chung, Y. S. (1988) Site-selective cAMP analogs at micromolar concentrations induce growth arrest and differentiation of acute promyelocytic, chronic myelocytic, and acute lymphocytic human leukemia cell lines. *Blood* **71,** 230–233
16. Rangarajan, S., Enserink, J. M., Kuiperij, H. B., de Rooij, J., Price, L. S., Schwede, F., and Bos, J. L. (2003) Cyclic AMP induces integrin-mediated cell adhesion through Epac and Rap1 upon stimulation of the beta 2-adrenergic receptor. *J. Cell Biol.* **160,** 487–493
17. Eid, A. H. (2012) cAMP induces adhesion of microvascular smooth muscle cells to fibronectin via an Epac-mediated but PKA-independent mechanism. *Cell. Physiol. Biochem.* **30,** 247–258
18. Enserink, J. M., Price, L. S., Methi, T., Mahic, M., Sonnenberg, A., Bos, J. L., and Tasken, K. (2004) The cAMP-Epac-Rap1 pathway regulates cell spreading and cell adhesion to laminin-5 through the alpha3beta1 integrin but not the alpha6beta4 integrin. *J. Biol. Chem.* **279,** 44889–44896
19. Lorenowicz, M. J., van Gils, J., de Boer, M., Hordijk, P. L., and Fernandez-Borja, M. (2006) Epac1-Rap1 signaling regulates monocyte adhesion and chemotaxis. *J. Leukoc. Biol.* **80,** 1542–1552
20. Badino, G. R., Novelli, A., Girardi, C., and Di Carlo, F. (1996) Evidence for functional beta-adrenoceptor subtypes in CG-5 breast cancer cell. *Pharmacol. Res.* **33,** 255–260
21. Slotkin, T. A., Zhang, J., Dancel, R., Garcia, S. J., Willis, C., and Seidler, F. J. (2000) Beta-adrenoceptor signaling and its control of cell replication in MDA-MB-231 human breast cancer cells. *Breast Cancer Res. Treat.* **60,** 153–166
22. Vandewalle, B., Revillion, F., and Lefebvre, J. (1990) Functional beta-adrenergic receptors in breast cancer cells. *J. Cancer Res. Clin. Oncol.* **116,** 303–306
23. Perez, P. C., Bruzzone, A., Sarappa, M., Castillo, L., and Luthy, I. (2012) Involvement of alpha2- and beta2-adrenoceptors on breast cancer cell proliferation and tumour growth regulation. *Br. J. Pharmacol.* **166,** 721–736
24. Draoui, A., Vandewalle, B., Hornez, L., Revillion, F., and Lefebvre, J. (1991) Beta-adrenergic receptors in human breast cancer: identification, characterization and correlation with progesterone and estradiol receptors. *Anticancer Res.* **11,** 677–680
25. Powe, D. G., Voss, M. J., Habashy, H. O., Zanker, K. S., Green, A. R., Ellis, I. O., and Entschladen, F. (2011) Alpha- and beta-adrenergic receptor (AR) protein expression is associated with poor clinical outcome in breast cancer: an immunohistochemical study. *Breast Cancer Res. Treat.* **130,** 457–463
26. Barron, T. I., Sharp, L., and Visvanathan, K. (2012) Beta-adrenergic blocking drugs in breast cancer: a perspective review. *Ther. Adv. Med. Oncol.* **4,** 113–125
27. Powe, D. G., Voss, M. J., Zanker, K. S., Habashy, H. O., Green, A. R., Ellis, I. O., and Entschladen, F. (2010) Beta-blocker drug therapy reduces secondary cancer formation in breast cancer and improves cancer specific survival. *Oncotarget* **1,** 628–638
28. Carie, A. E., and Sebti, S. M. (2007) A chemical biology approach identifies a beta-2 adrenergic receptor agonist that causes human tumor regression by blocking the Raf-1/Mek-1/Erk1/2 pathway. *Oncogene* **26,** 3777–3788
29. Sloan, E. K., Priceman, S. J., Cox, B. F., Yu, S., Pimentel, M. A., Tangkanangnukul, V., Arevalo, J. M., Morizono, K., Karanikolas, B. D., Wu, L., Sood, A. K., and Cole, S. W. (2010) The sympathetic nervous system induces a metastatic switch in primary breast cancer. *Cancer Res.* **70,** 7042–7052
30. Spina, A., Di Maiolo, F., Esposito, A., Sapio, L., Chiosi, E., Sorvillo, L., and Naviglio, S. (2012) cAMP elevation downregulates beta3 integrin and focal adhesion kinase and inhibits leptin-induced migration of MDA-MB-231 breast cancer cells. *Biores. Open Access* **1,** 324–332
31. Wellner, R. B., He, X. J., Marmary, Y., and Baum, B. J. (1988) Functional beta-adrenergic receptors in a human mammary cell line (HBL-100). *Biochem. Pharmacol.* **37,** 3035–3037
32. Sauliere, A., Bellot, M., Paris, H., Denis, C., Finana, F., Hansen, J. T., Altie, M. F., Seguelas, M. H., Pathak, A., Hansen, J. L., Senard, J. M., and Gales, C. (2012) Deciphering biased-agonism complexity reveals a new active AT1 receptor entity. *Nat. Chem. Biol.* **8,** 622–630
33. Livak, K. J., and Schmittgen, T. D. (2001) Analysis of relative gene expression data using real-time quantitative PCR and the 2(-delta delta C(T)) method. *Methods* **25,** 402–408

34. Gilman, A. G. (1970) A protein binding assay for adenosine 3′:5′-cyclic monophosphate. *Proc. Natl. Acad. Sci. U. S. A.* **67,** 305–312
35. Shenoy, S. K., Drake, M. T., Nelson, C. D., Houtz, D. A., Xiao, K., Madabushi, S., Reiter, E., Premont, R. T., Lichtarge, O., and Lefkowitz, R. J. (2006) beta-arrestin-dependent, G protein-independent ERK1/2 activation by the beta2 adrenergic receptor. *J. Biol. Chem.* **281,** 1261–1273
36. Gjertsen, B. T., Mellgren, G., Otten, A., Maronde, E., Genieser, H. G., Jastorff, B., Vintermyr, O. K., McKnight, G. S., and Doskeland, S. O. (1995) Novel (Rp)-cAMPS analogs as tools for inhibition of cAMP-kinase in cell culture. Basal cAMP-kinase activity modulates interleukin-1 beta action. *J. Biol. Chem.* **270,** 20599–20607
37. Almahariq, M., Tsalkova, T., Mei, F. C., Chen, H., Zhou, J., Sastry, S. K., Schwede, F., and Cheng, X. (2013) A novel EPAC-specific inhibitor suppresses pancreatic cancer cell migration and invasion. *Mol. Pharmacol.* **83,** 122–128
38. Castellone, M. D., Teramoto, H., Williams, B. O., Druey, K. M., and Gutkind, J. S. (2005) Prostaglandin E2 promotes colon cancer cell growth through a Gs-axin-beta-catenin signaling axis. *Science* **310,** 1504–1510
39. Hochbaum, D., Tanos, T., Ribeiro-Neto, F., Altschuler, D., and Coso, O. A. (2003) Activation of JNK by Epac is independent of its activity as a Rap guanine nucleotide exchanger. *J. Biol. Chem.* **278,** 33738–33746
40. Ostrom, R. S., and Insel, P. A. (2004) The evolving role of lipid rafts and caveolae in G protein-coupled receptor signaling: implications for molecular pharmacology. *Br. J. Pharmacol.* **143,** 235–245
41. Mouat, M. F., Greenspan, P., Byerley, L. O., and Grider, A. (2003) Zinc uptake into MCF-10A cells is inhibited by cholesterol depletion. *J. Nutr. Biochem.* **14,** 74–80
42. Sun, Y., Huang, J., Xiang, Y., Bastepe, M., Juppner, H., Kobilka, B. K., Zhang, J. J., and Huang, X. Y. (2007) Dosage-dependent switch from G protein-coupled to G protein-independent signaling by a GPCR. *EMBO J.* **26,** 53–64
43. Swaminath, G., Xiang, Y., Lee, T. W., Steenhuis, J., Parnot, C., and Kobilka, B. K. (2004) Sequential binding of agonists to the beta2 adrenoceptor. Kinetic evidence for intermediate conformational states. *J. Biol. Chem.* **279,** 686–691
44. Guzzi, F., Zanchetta, D., Cassoni, P., Guzzi, V., Francolini, M., Parenti, M., and Chini, B. (2002) Localization of the human oxytocin receptor in caveolin-1 enriched domains turns the receptor-mediated inhibition of cell growth into a proliferative response. *Oncogene* **21,** 1658–1667
45. Leitinger, B., and Hogg, N. (2002) The involvement of lipid rafts in the regulation of integrin function. *J. Cell Sci.* **115,** 963–972
46. Zocher, M., Zhang, C., Rasmussen, S. G., Kobilka, B. K., and Muller, D. J. (2012) Cholesterol increases kinetic, energetic, and mechanical stability of the human beta2-adrenergic receptor. *Proc. Natl. Acad. Sci. U. S. A.* **109,** E3463–3472
47. Pontier, S. M., Percherancier, Y., Galandrin, S., Breit, A., Gales, C., and Bouvier, M. (2008) Cholesterol-dependent separation of the beta2-adrenergic receptor from its partners determines signaling efficacy: insight into nanoscale organization of signal transduction. *J. Biol. Chem.* **283,** 24659–24672
48. Xiang, Y., Rybin, V. O., Steinberg, S. F., and Kobilka, B. (2002) Caveolar localization dictates physiologic signaling of beta 2-adrenoceptors in neonatal cardiac myocytes. *J. Biol. Chem.* **277,** 34280–34286
49. Kassel, K. M., Wyatt, T. A., Panettieri, R. A., Jr., and Toews, M. L. (2008) Inhibition of human airway smooth muscle cell proliferation by beta 2-adrenergic receptors and cAMP is PKA independent: evidence for EPAC involvement. *Am. J. Physiol. Lung Cell. Mol. Physiol.* **294,** L131–138
50. Brock, M., Nickel, A. C., Madziar, B., Blusztajn, J. K., and Berse, B. (2007) Differential regulation of the high affinity choline transporter and the cholinergic locus by cAMP signaling pathways. *Brain Res.* **1145,** 1–10
51. Kiermayer, S., Biondi, R. M., Imig, J., Plotz, G., Haupenthal, J., Zeuzem, S., and Piiper, A. (2005) Epac activation converts cAMP from a proliferative into a differentiation signal in PC12 cells. *Mol. Biol. Cell* **16,** 5639–5648
52. Dodge-Kafka, K. L., Soughayer, J., Pare, G. C., Carlisle Michel, J. J., Langeberg, L. K., Kapiloff, M. S., and Scott, J. D. (2005) The protein kinase A anchoring protein mAKAP coordinates two integrated cAMP effector pathways. *Nature* **437,** 574–578
53. Honegger, K. J., Capuano, P., Winter, C., Bacic, D., Stange, G., Wagner, C. A., Biber, J., Murer, H., and Hernando, N. (2006) Regulation of sodium-proton exchanger isoform 3 (NHE3) by PKA and exchange protein directly activated by cAMP (EPAC). *Proc. Natl. Acad. Sci. U. S. A.* **103,** 803–808
54. Cooper, D. M. (2005) Compartmentalization of adenylate cyclase and cAMP signalling. *Biochem. Soc. Trans.* **33,** 1319–1322
55. Houslay, M. D. (2010) Underpinning compartmentalised cAMP signalling through targeted cAMP breakdown. *Trends Biochem. Sci.* **35,** 91–100
56. Agarwal, S. R., MacDougall, D. A., Tyser, R., Pugh, S. D., Calaghan, S. C., and Harvey, R. D. (2011) Effects of cholesterol depletion on compartmentalized cAMP responses in adult cardiac myocytes. *J. Mol. Cell. Cardiol.* **50,** 500–509
57. Wu, C. Y., DiJulio, D. H., Jacobson, K. L., McKnight, G. S., and Watson, E. L. (2010) The contribution of AKAP5 in amylase secretion from mouse parotid acini. *Am. J. Physiol. Cell Physiol.* **298,** C1151–C1158
58. De Arcangelis, V., Liu, S., Zhang, D., Soto, D., and Xiang, Y. K. (2010) Equilibrium between adenylyl cyclase and phosphodiesterase patterns adrenergic agonist dose-dependent spatiotemporal cAMP/protein kinase A activities in cardiomyocytes. *Mol. Pharmacol.* **78,** 340–349
59. Zaccolo, M., Cesetti, T., Di Benedetto, G., Mongillo, M., Lissandron, V., Terrin, A., and Zamparo, I. (2005) Imaging the cAMP-dependent signal transduction pathway. *Biochem. Soc. Trans.* **33,** 1323–1326
60. Inderwies, T., Pfaffl, M. W., Meyer, H. H., Blum, J. W., and Bruckmaier, R. M. (2003) Detection and quantification of mRNA expression of alpha- and beta-adrenergic receptor subtypes in the mammary gland of dairy cows. *Domest. Anim. Endocrinol.* **24,** 123–135
61. Marchetti, B., Fortier, M. A., Poyet, P., Follea, N., Pelletier, G., and Labrie, F. (1990) Beta-adrenergic receptors in the rat mammary gland during pregnancy and lactation: characterization, distribution, and coupling to adenylate cyclase. *Endocrinology* **126,** 565–574
62. Bos, J. L. (2003) Epac: a new cAMP target and new avenues in cAMP research. *Nat. Rev. Mol. Cell Biol.* **4,** 733–738
63. Enserink, J. M., Christensen, A. E., de Rooij, J., van Triest, M., Schwede, F., Genieser, H. G., Doskeland, S. O., Blank, J. L., and Bos, J. L. (2002) A novel Epac-specific cAMP analogue demonstrates independent regulation of Rap1 and ERK. *Nat. Cell Biol.* **4,** 901–906

Received for publication July 22, 2013.
Accepted for publication November 26, 2013.

Supplementary Figure 1

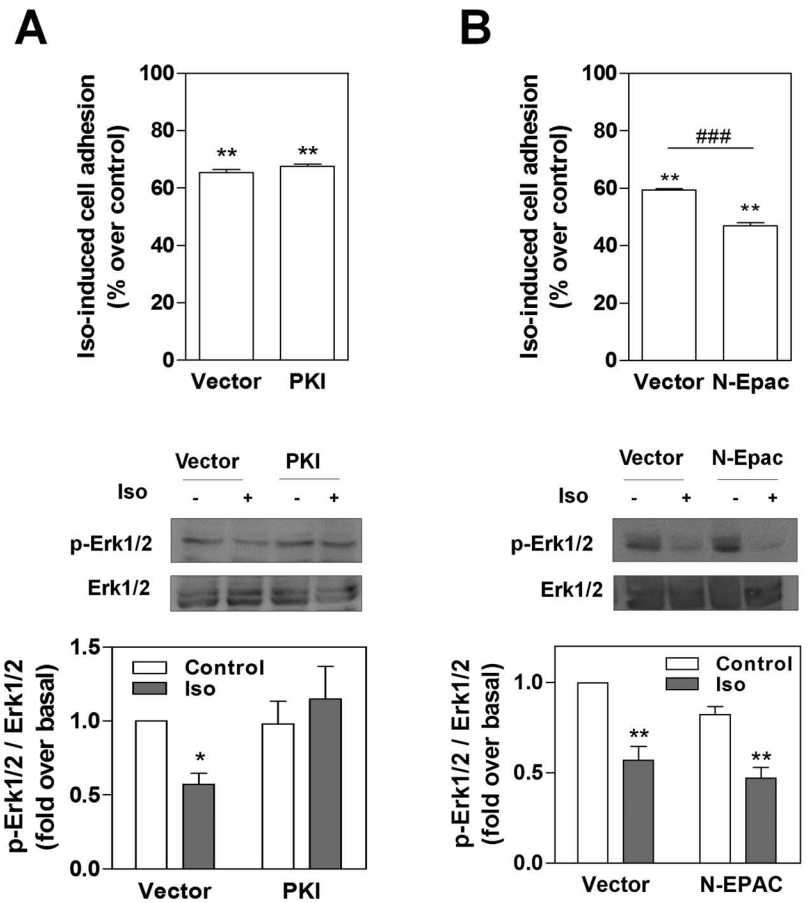

Supplementary Figure 1. β_2-AR mediates proliferation inhibition and adhesion stimulation of MCF-10A cells through PKA and Epac respectively. MCF-10A cells transiently overexpressing (**A**) PKA competitor (PKI) or (**B**) Epac competitor (N-Epac) or empty vector (vector) were stimulated or not (control) with 0.1 µM isoproterenol (Iso) during 15 min for cell adhesion (top panels) or 20 min for the evaluation of p-Erk1/2 inhibition (bottom panels). Data represent the mean ± s.e.m. of three to four independent experiments each performed in triplicates. Statistical significance was assessed using ANOVA followed by Bonferroni test. *p<0.05, **p<0.01 between stimulated and control cells. ### p<0.001 between N-Epac and Vector stimulated cells.

Supplementary Figure 2

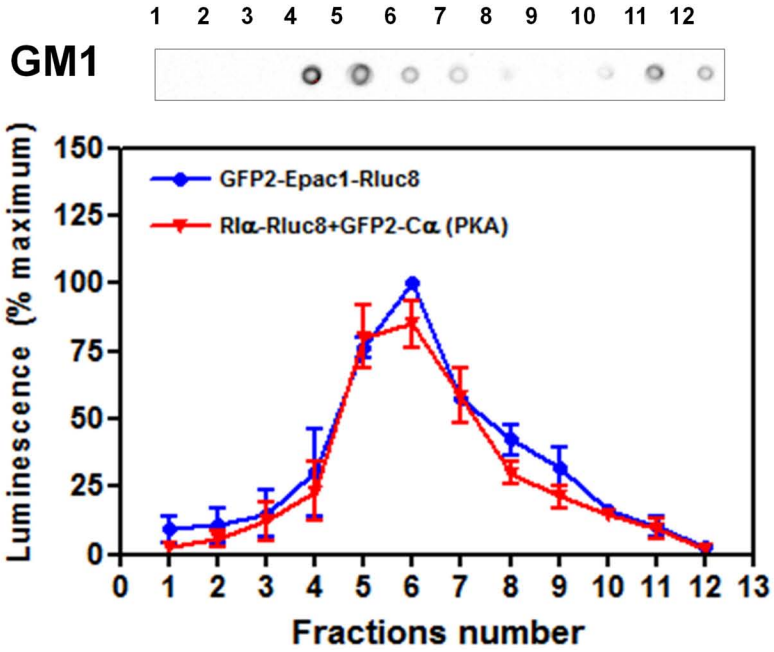

Supplementary Figure 2. PKA and Epac BRET-probes membrane distribution following preparation of low density membranes. Low density membranes of MCF-10A cells transiently expressing BRET biosensors RIα-Rluc8 and GFP2-Cα or GFP2-Epac1-Rluc8 were directly purified using a triton X-100 lysis followed by a separation on sucrose gradient. Detection of PKA or Epac probes was carried out by measuring total luminescence in each sucrose fraction. GM1 ganglioside (raft marker) was detected by dot-blot using peroxydase-coupled CTx (upper panel). Data are expressed as the percentage of the maximal luminescence detected in the sucrose fraction and represent the mean ± s.e.m. of three independent experiments.